ACS Chemical Neuroscience

Research Article

pubs.acs.org/chemneuro

# Targeting the Cyclophilin Domain of Ran-binding Protein 2 (Ranbp2) with Novel Small Molecules to Control the Proteostasis of STAT3, hnRNPA2B1 and M-Opsin

Kyoung-in Cho,[†] Andrew Orry,[‡] Se Eun Park,[†] and Paulo A. Ferreira*[,†,§]

[†]Department of Ophthalmology, Duke University Medical Center, Durham, North Carolina 27710, United States

[‡]MolSoft LLC, San Diego, California 92121, United States

[§]Department of Pathology, Duke University Medical Center, Durham, North Carolina 27710, United States

**ABSTRACT:** Cyclophilins are peptidyl *cis*−*trans* prolyl isomerases (PPIases), whose activity is typically inhibited by cyclosporine A (CsA), a potent immunosuppressor. Cyclophilins are also chaperones. Emerging evidence supports that cyclophilins present nonoverlapping PPIase and chaperone activities. The proteostasis of the disease-relevant substrates, signal transducer and activator of transcription 3 and 5 (STAT3/STAT5), heterogeneous nuclear ribonucleoprotein A2B1 (hnRNPA2B1), and M-opsin, is regulated by nonoverlapping chaperone and PPIase activities of the cyclophilin domain (CY) of Ranbp2, a multifunctional and modular scaffold that controls nucleocytoplasmic shuttling and proteostasis of selective substrates. Although highly homologous, CY and the archetypal cyclophilin A (CyPA) present distinct catalytic and CsA-binding activities owing to unique structural features between these cylophilins. We explored structural idiosyncrasies between CY and CyPA to screen *in silico* nearly 9 million small molecules (SM) against the CY PPIase pocket and identify SMs with selective bioactivity toward STAT3, hnRNPA2B1, or M-opsin proteostasis. We found three classes of SMs that enhance the cytokine-stimulated transcriptional activity of STAT3 without changing latent and activated STAT3 levels, down-regulate hnRNPA2B1 or M-opsin proteostasis, or a combination of these. Further, a SM that suppresses hnRNPA2B1 proteostasis also inhibits strongly and selectively the PPIase activity of CY. This study unravels chemical probes for multimodal regulation of CY of Ranbp2 and its substrates, and this regulation likely results in the allosterism stemming from the interconversion of conformational substates of cyclophilins. The results also demonstrate the feasibility of CY in drug discovery against disease-relevant substrates controlled by Ranbp2, and they open new opportunities for therapeutic interventions.

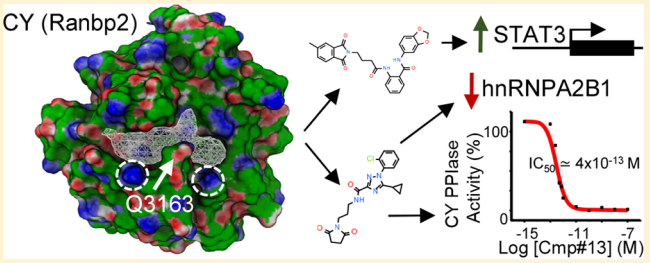


**KEYWORDS:** *Ran-binding protein 2 (Ranbp2), cyclophilin, chaperone, proteostasis, hnRNPA2B1, STAT3, M-opsin, chemical ligands*

Cyclophilins are members of peptidyl *cis*−*trans* prolyl isomerases (PPIases),[1−3] whose activity promotes protein folding or conformational switches in protein signaling.[4−6] Cyclophilins also bind the cyclic undecapeptide and potent immunosuppressor drug, cyclosporine A (CsA).[7−9] Cyclophilin A (CyPA or PPIA), a prototypical member of the cyclophilin family, mediates immunosuppression,[9,10] and nonimmunosuppressor structural variants of CsA have been exploited in the treatment of diseases,[9,11,12] such as infections caused by HIV-1 and HCV.[13−18]

Cyclophilins act also as chaperones. For example, the cyclophilin encoded by *ninaA* of *Drosophila* chaperones the biogenesis of selective opsins of photoreceptor neurons.[19−21] The molecular bases of the chaperone activity of NinaA and other cyclophilins remain unclear; however, mutational or structural studies of NinaA,[5] CyPH/PPIL1,[22−24] or CyPB (PPIB)[25] support that this activity arises from the stable association of substrates to binding sites in cyclophilin that do not overlap with its PPIase site and that are not affected by CsA binding. This notion of mutually exclusive sites in cyclophilins toward distinct substrates was strengthened by the findings that the cyclophilin domain (CY) of Ranbp2 harbors selective physiological activities toward four disease-relevant substrates, STAT3/STAT5, hnRNPA2B1 and M-opsin.[26] Ranbp2 is a large 358 kDa multimodular, pleiotropic, and cytoplasmic peripheral nucleoporin, which is not exclusively localized at nuclear pores.[26−31] Selective domains of Ranbp2 control nucleocytoplasmic trafficking,[28,31−37] sumoylation,[38−40] microtubule-based motor activity of kinesin-1,[41−43] and proteostasis of selective proteins.[26,44−47] In particular, M-opsin biogenesis is dependent on the C-terminal chaperone activity of CY but not on CY PPIase activity.[26] By contrast, loss of CY PPIase activity down-regulates the proteostasis of hnRNPA2B1, whereas impairments of CY PPIase and C-terminal chaperone activities lack apparently untoward effects of CY association with latent and stress-activated STAT3/STAT5.[26] Regulation of proteo-

**Received:** May 10, 2015
**Accepted:** June 1, 2015
**Published:** June 1, 2015





DOI: 10.1021/acschemneuro.5b00134
*ACS Chem. Neurosci.* 2015, 6, 1476−1485

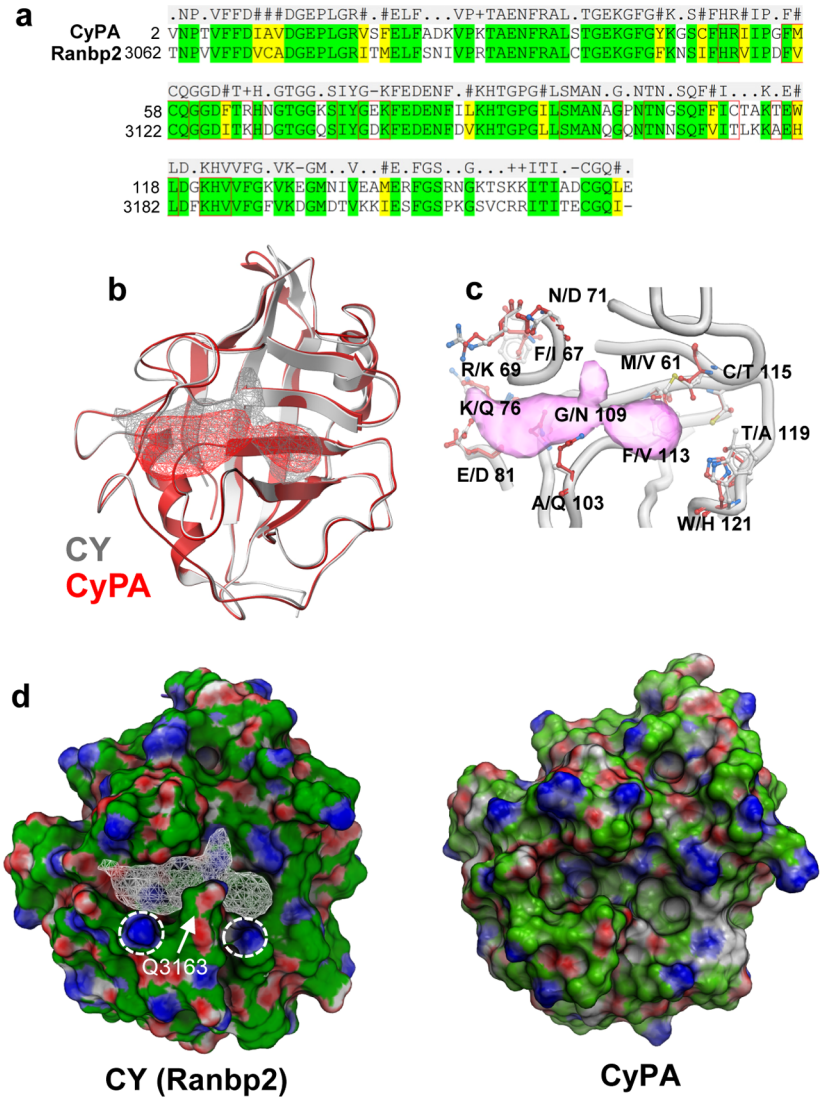


**Figure 1.** Heterogeneity of structural ensembles between the PPIase pockets of CY of Ranbp2 and CyPA. (a) Amino acid sequence alignment of CY of Ranbp2 and cyclophilin A (CyPA). CY and CyPA are 65% identical. Residues within 7 Å of the PPIase pocket are noted within red line boxes. (b) Ribbon representation of superposition of CY of Ranbp2 (gray) and CyPA (red). Mesh represents extended PPIase pocket of CY (gray) and that of CyPA (red). (c) Nonconserved residues of the PPIase/CsA-binding pockets of CyPA (listed first) and CY of Ranbp2 (listed second). Extended CY PPIase pocket is in pink. Numbering refers CyPA residues. (d) Surface representations of CY of Ranbp2 and CyPA colored by qualitative electrostatic potential calculated by ICM using a color scale from red to blue and values of ±5 kcal/electron units (+5 = blue, −5 = red). The conserved K3142 and K3185 (circles) and the nonconserved Q3163 residues of CY (arrow) and its PPIase pocket (white mesh) are shown. Variable orientations of side chains of K3142 and K3185 of CY of Ranbp2 and equivalent residues in CyPA cause surface electrostatic shifts.

stasis of substrates by CY activities is important, because STAT3/STAT5 misregulation is linked to inflammation, cancer, and neurodegeneration,[48−55] aggregation-prone mutations in *hnRNPA2B1* cause multisystem proteinopathies (MSPs) and amyotrophic lateral sclerosis (ALS),[56] and those in L/M-opsins (*OPN1LW/OPN1MW*) lead to cone photoreceptor neuron dystrophy and color blindness.[57] Mounting evidence also supports that HIV-1 usurps the PPIase activity of CY of Ranbp2. The binding and prolyl isomerization of the CyPA-binding loop of HIV-1 capsid to CY of Ranbp2 uncoats and promotes nuclear entry of HIV-1.[15,58]

Recent data support that the archetypal CyPA undergoes conformational fluctuations leading to side-chain conformational heterogeneity in residues unrelated and related to catalysis.[3,59−61] For example, alternative side-chain rotamers, such as Phe113 at the base of the PPIase pocket, can cause long-range chemical shifts.[59] These critical data establish a direct relationship between rates of conformational substates of CyPA and catalysis. The dynamic properties of CyPA are likely extended to other cyclophilin members, such as CY of Ranbp2. For example, CY can undergo phosphorylation of residues away from the PPIase site and this modification reduces the PPIase activity of CY.[26] Collectively, these data support that cyclophilins interconvert between conformational substates and that distinct structural ensembles of cyclophilins are coupled directly to unique function(s). Importantly, these mechanisms may be explored to modulate pharmacologically and selectively manifold activities of cyclophilins on their substrates.

Here, we explored the heterogeneity of structural ensembles between the PPIase pockets of CY of Ranbp2 and its closest homologue, CyPA, to screen nearly 9 million small molecules


DOI: 10.1021/acschemneuro.5b00134
*ACS Chem. Neurosci.* 2015, 6, 1476−1485

and discover unique chemical probes selective to CY that modulate distinct features of proteostasis of CY substrates, STAT3, hnRNPA2B1 and M-opsin.

## RESULTS AND DISCUSSION

**Exploring the Structural Heterogeneity of CY and CyPA for *in Silico* Screening of Chemical Ligands of CY.** The primary sequence of CY of Ranbp2 is 65% identical to CyPA (Figure 1a).[29] Comparison between the available PDB crystal structures of the PPIase pockets of CY and CyPA indicates that CY harbors an extended PPIase pocket with an area and volume of 370 Å$^2$ and 357 Å$^3$ compared with 301 Å$^2$ and 312 Å$^3$ of CyPA, respectively (Figure 1b). Further, several critical residues within or surrounding the PPIase pocket were unique to CY of Ranbp2. For example, A103 and W121 in CyPA are replaced by Q3163 and H3181 in CY of Ranbp2, respectively (Figure 1c). These highly conserved residues among cyclophilins[29] are critical to CsA binding to CyPA. Q3163 is predicted to restrict binding of CsA to CY, whereas the mutations W121F and W121A in CyPA were shown to decrease 75- and 200-fold their binding activities to CsA and 2- and 13-fold their catalytic efficiencies ($k_{cat}/K_m$), respectively.[62] Conversely, replacement of the equivalent residue H141W of CyP40 increases its catalytic efficiency and binding to CsA.[63] Hence, the nonconserved Q3163 and H3181 residues in CY of Ranbp2 are thought to contribute to its decreased catalytic efficiency on standard peptidyl-prolyl substrates and CsA-binding activity.[26,29] In addition to other conservative and nonconservative substitutions in CY PPIase pocket (Figure 1c), CyPA and CY present also surface electrostatic changes owing to differences of orientation of side chains of conserved lysines toward or away from the PPIase pocket (e.g., K3142 (K82 in CyPA) and K3185 (K125 in CyPA); Figure 1c,d) and whose acetylation in CyPA promotes surface electrostatic shifts and PPIase inhibition.[64,65]

We took advantage of the structure of CY determined at 1.75 Å (PDB 4I9Y)[64] and unique structural ensembles between the PPIase pockets of CY and CyPA (PDB 2CPL)[66] (Figure 1c) to screen a library of nearly 9 million small molecules against the extended CY PPIase pocket with structure-based and virtual ligand screening (VLS) approaches (Figure 2). These approaches produced 679 potential ligands to the PPIase pocket of CY of Ranbp2 after counter-screening ligand candidates of CY against the PPIase pocket of CyPA (Figure 2). Fourteen high-scoring compounds against the atomic structure of CY determined at 1.75 Å (PDB 4I9Y) were selected for experimental analysis upon visual inspection of various structural features, such as geometries, functional groups, and interactions with the receptor. Figure 3 shows the chemical structures of six of the 14 candidate ligands of CY and that were found in this study to show pharmacological activity toward physiological substrates of CY of Ranbp2. Compounds without CY pharmacological activity likely represent false positives from the *in silico* screening owing to the lack of the incorporation of dynamics of CY and absence of multiple atomic structures of CY.

**Modulation of STAT3-Transcriptional Activity by Chemical Ligands of CY.** Chemical compounds were assessed for their ability to modulate STAT3 transcriptional activity. We chose a STAT3 luciferase reporter HeLa stable cell line to screen the compounds, because this cell line lacks endogenous activated STAT3 in the absence of the cytokine oncostatin-M (OncM), but robust STAT3 activation (STAT3-

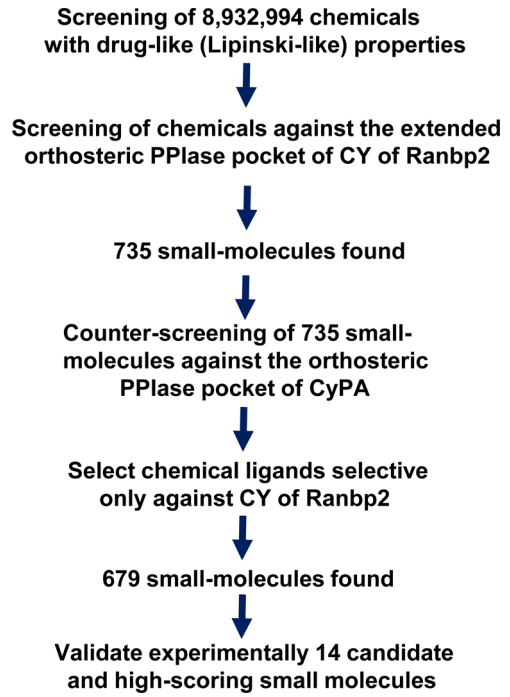


**Figure 2.** Diagram of strategy for structure-based ligand screening *in silico* of candidate small molecules against the PPIase pocket of CY of Ranbp2.

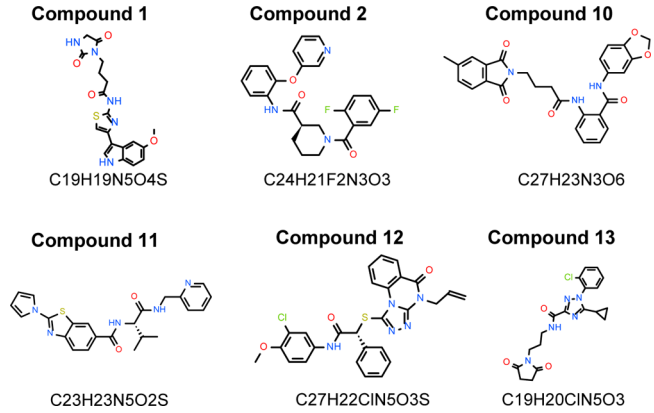


**Figure 3.** Chemical structures of bioactive ligands of CY PPIase pocket identified by *in silico* screening and examined by this study experimentally. Compound **1**, 4-(2,5-dioxo-imidazolidin-1-yl)-*N*-[4-(5-methoxy-1H-indol-3-yl)-thiazol-2-yl]-butyramide; compound **2**, 1-(2,5-difluorobenzoyl)-*N*-[2-(3-pyridinyloxy)phenyl]-3-piperidinecarboxamide; compound **10**, *N*-(2*H*-1,3-benzodioxol-5-yl)-2-[4-(5-methyl-1,3-dioxo-2,3-dihydro-1*H*-isoindol-2-yl)butanamido]benzamide; compound **11**, (*S*)-*N*-(3-methyl-1-oxo-1-((pyridin-2-ylmethyl)amino)-butan-2-yl)-2-(1*H*-pyrrol-1-yl)benzodthiazole-6-carboxamide; compound **12**, *N*-(3-chloro-4-methoxyphenyl)-2-{[5-oxo-4-(prop-2-en-1-yl)-4*H*,5*H*-[1,2,4]triazolo[4,3-*a*]quinazolin-1-yl]sulfanyl}-2-phenylacetamide; compound **13**, 1-(2-chlorophenyl)-5-cyclopropyl-*N*-[3-(2,5-dioxopyrrolidin-1-yl)propyl]-1*H*-1,2,4-triazole-3-carboxamide.

(P)) ensues upon OncM stimulation (Figure 4a,b). By contrast, IL-6 had no effect on STAT3-transcriptional activity (Figure 4b). Further, this line endogenously expresses hnRNPA2B1 and Ranbp2, whose levels remain unchanged by the absence or presence of OncM (Figure 4a).

We examined the dose response of STAT3-transcriptional activation in the presence of increasing concentrations of chemical compounds. As shown in Figure 4c, we found that


DOI: 10.1021/acschemneuro.5b00134
ACS Chem. Neurosci. 2015, 6, 1476−1485

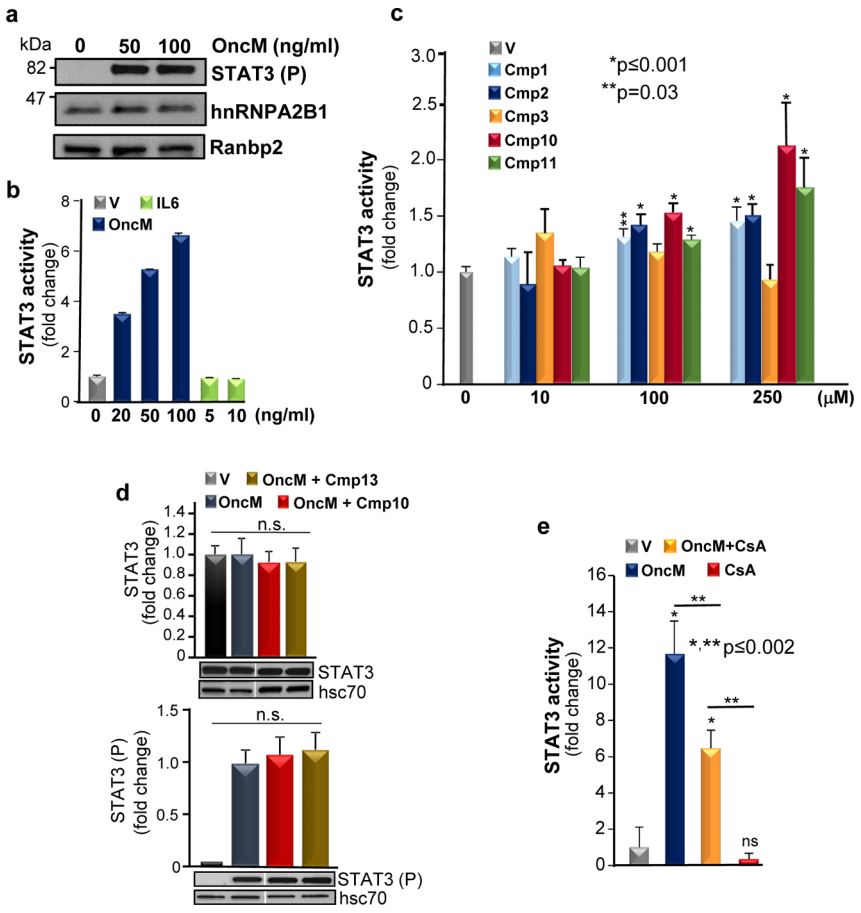


**Figure 4.** Pharmacological properties of CY chemical ligands in STAT3 transcriptional activation potential. (a) Immunoblots of STAT3(P) (activated STAT3) from homogenates of STAT3 luciferase reporter HeLa stable cell line treated or untreated with oncostatin M (OncM). Levels of hnRNPA2B1 and Ranbp2 remain unchanged between OncM untreated and treated cells. (b) Luciferase activity induced by STAT3-transcriptional activation in the absence or presence of OncM and IL-6. (c) Dose-dependent responses of STAT3-transcriptional activity of STAT3 luciferase reporter HeLa stable cells treated with OncM in the absence and presence of small molecules (Cmp). (d) Levels of latent STAT3 and activated STAT3(P) remain unchanged in the absence or presence of small molecules with (e.g., Cmp 10) and without effect (e.g., Cmp 13) on OncM-stimulated STAT3 activity. (e) CsA suppresses the STAT3-transcriptional activity stimulated by OncM. Data shown represent the mean ± sd, $n = 3$ (b, c, d, e); ns, nonsignificant. Legend: V, vehicle; Cmp, compound (small molecule).

four chemicals, compounds **1**, **2**, **10**, and **11**, enhanced STAT3-transcriptional activity and among these compound **10** had the strongest effect (>2-fold increase). By contrast, compound **3** (Figure 4c) and other compounds had no effect (data not shown). Interestingly, compound **1** was extremely labile because its bioactivity was completely lost upon solvation and short-term storage. Conversely, compound **14** was cytotoxic and was not included for further analysis. Finally, the enhancement of STAT3-transcriptional activity was not caused by changes in the levels of latent and activated STAT3, because the levels of STAT3 and STAT3(P) were unchanged in the absence and presence of the compounds with and without effects on STAT3-transcriptional activity (Figure 4d).

CyPA and CyPB bind to CsA, and this association promotes the down-regulation of STAT3-transcriptional activity.[67] To probe the selectivity of the mechanisms of regulation of STAT3-transcriptional activation, we treated cells with CsA in the absence and presence of OncM. In comparison to unchallenged HeLa cells, CsA had no effect on STAT3 activation. However, CsA reduced by ∼50% the levels of STAT3-transcriptional activity upon treatment of cells with OncM (Figure 4e). Hence, CsA and compounds **1**, **2**, **10**, and **11** elicit contrasting effects in STAT3-transcriptional activation.

**Modulation of hnRNPA2B1 Proteostasis by Chemical Ligands of CY.** To assess the effect of the chemical compounds toward CY in hnRNPA2B1 proteostasis, the STAT3 luciferase reporter HeLa stable cell line was cultured without cytokine challenge in the absence and presence of the compounds. As shown in Figure 5a (upper panel), compounds **11**−**13** elicited strong down-regulation of hnRNPA2B1 levels. Quantitative analyses of immunoblots showed that compounds **11**−**13** elicited a greater than 2-fold reduction of hnRNPA2B1 levels, whereas compounds **1** and **10**, and all other compounds, had milder and no effects in hnRNPA2B1 proteostasis, respectively (Figure 5a, lower panel). Finally, there was also a dose-dependent response of hnRNPA2B1 down-regulation toward compound **11** (Figure 5b).

**Modulation of M-opsin by Chemical Ligands of CY.** We used a transformed cone photoreceptor line, which expresses endogenously M-opsin,[68,69] to ascertain the effect on M-opsin proteostasis of compounds without overlapping effects in STAT3-transcriptional activation and regulation of hnRNPA2B1 proteostasis, such as compounds **2** and **13**. As shown in Figure 5c, compounds **2** and **13** exerted mild but contrasting and significant effects in M-opsin proteostasis.


DOI: 10.1021/acschemneuro.5b00134
ACS Chem. Neurosci. 2015, 6, 1476−1485

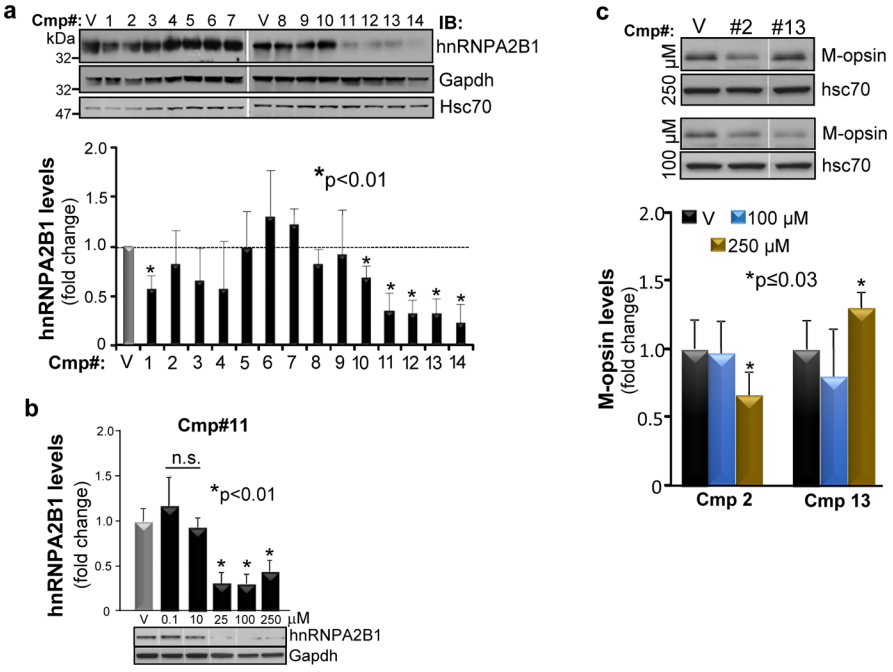


**Figure 5.** Pharmacological effects of CY chemical ligands in hnRNPA2B1 and M-opsin proteostasis. (a) Immunoblot (top panel) and quantitative analyses (lower panel) of hnRNPA2B1 levels in homogenates of STAT3 luciferase reporter HeLa stable cells untreated and treated with small molecules (100 $\mu$M). Compounds **11**–**13** strongly reduce hnRNPA2B1 levels. Compound **14** is cytotoxic. (b) Quantitative analyses (upper graph) by immunoblot of hnRNPA2B1 levels (lower panel) in homogenates of HeLa cells untreated and treated with increasing concentrations of compound **11**. (c) Immunoblot (upper panel) and quantitative analyses (lower panel) of M-opsin levels in homogenates of 661W cells untreated and treated with small molecules. Compounds **2** and **13** reduce and increase M-opsin levels, respectively. Data shown represent the mean ± sd, $n$ = 4 (a–c). Legend: V, vehicle (compound solvent) only; Cmp, compound (small molecule); Gapdh, Glyceraldehyde 3-phosphate dehydrogenase; hsc70, cytosolic heat shock cognate protein 70.

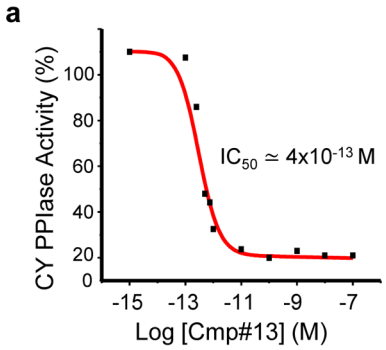


b

| | $k_{cat}/K_m$ ($mM^{-1}s^{-1}$) |
|---|---|
| CyPA | 1544.6 ± 229.4 |
| CyPA + CsA | 20.6 ± 21.0 |
| CyPA + Cmp13 | 1694.0 ± 370.4 |
| CY | 142.9 ± 43.3 |
| CY + CsA | 148.3 ± 60.1 |
| CY + Cmp13 | 25.5 ± 8.6 |

**Figure 6.** Inhibitory effects of compound **13** and CsA on CY and CyPA PPIase activities. (a) Direct inhibition of PPIase activity of CY by compound **13**. Compound **13** has an $IC_{50}$ of ~$4 \times 10^{-13}$ M on the catalytic efficiency ($k_{cat}/K_m$) of CY. (b) Inhibitory effects of CsA and compound 13 on the catalytic efficiency of CyPA and CY of Ranbp2. Data shown represent the mean ± sd, $n$ = 4–6 (b). Legend: V, vehicle; Cmp, compound (small molecule).

Compounds **2** and **13** selectively decreased and increased M-opsin levels, respectively.

**Inhibition of CY PPIase Activity by Chemical Compounds.** CY of Ranbp2 harbors nonoverlapping PPIase and chaperone activities toward STAT3/STAT5, hnRNPA2B1, and M-opsin, and CY likely adopts conformational substates with inherent effects on CY functions and PPIase activity.[26] To discern further the mechanisms of compounds **1**–**13** in CY functions, we measured the direct effects of these compounds on CY PPIase activity. Among these compounds, only compound **13** had a potent and selective inhibitory effect on CY PPIase activity. As shown in Figure 6a, the $IC_{50}$ of compound **13** for CY of Ranbp2 was ~$4 \times 10^{-13}$ M. In addition, we evaluated the selectivity of compound **13** and CsA toward the PPIase activities of CyPA and CY at known saturating PPIase inhibitory concentrations of compound **13** (this study, Figure 6a) and CsA for CY and CyPA, respectively.[62,65] As shown in Figure 6b, 100 nM of CsA strongly inhibited the PPIase activity of CyPA but had no effect on CY PPIase activity. By contrast, compound **13** did not inhibit the PPIase activity of CyPA. Hence, compound **13** is a novel, potent, and highly selective orthosteric inhibitor of the PPIase activity of CY of Ranbp2.

**Distinctive Features of CY–Ligand Complexes.** To gain insights to the structural bases for the pharmacological and biochemical effects between the compounds described in this study, we examined the poses of the ligands docked in the extended PPIase pocket of Ranbp2. We modeled and calculated


DOI: 10.1021/acschemneuro.5b00134
ACS Chem. Neurosci. 2015, 6, 1476–1485

a

| CY (Ranbp2) | CyPA | CY + Cmp1 | CY + Cmp2 | CY + Cmp10 | CY + Cmp11 | CY + Cmp12 | CY + Cmp13 | CyPA + CsA |
|---|---|---|---|---|---|---|---|---|
| H3114 | H54 | 0.00 | 14.04 | 4.11 | 10.96 | 13.72 | 9.43 | 0.00 |
| R3115 | R55 | 24.39 | 30.64 | 36.88 | 35.91 | 25.12 | 36.76 | 41.24 |
| I3117 | I57 | 0.00 | 0.00 | 0.00 | 0.00 | 0.00 | 0.00 | 2.20 |
| F3120 | F60 | 16.64 | 11.31 | 21.63 | 11.59 | 0.32 | 20.39 | 38.83 |
| **V3121** | M61 | 0.00 | 4.10 | 0.00 | 6.93 | 0.00 | 1.89 | 9.82 |
| Q3123 | Q63 | 16.07 | 24.32 | 21.05 | 24.39 | 16.17 | 25.68 | 20.59 |
| **D3131** | N71 | 0.00 | 0.00 | 2.40 | 0.48 | 11.18 | 0.00 | 0.00 |
| G3132 | G72 | 15.13 | 19.10 | 25.28 | 21.93 | 25.35 | 17.62 | 18.16 |
| T3133 | T73 | 25.70 | 2.52 | 11.17 | 17.52 | 24.95 | 13.39 | 7.77 |
| G3134 | G74 | 5.00 | 2.62 | 11.17 | 15.04 | 12.75 | 4.04 | 0.00 |
| G3135 | G75 | 0.00 | 0.00 | 0.00 | 6.02 | 0.24 | 0.00 | 0.00 |
| **D3141** | E81 | 0.00 | 0.00 | 0.00 | 10.43 | 0.00 | 0.00 | 0.00 |
| K3142 | K82 | 0.00 | 0.00 | 0.63 | 8.48 | 0.00 | 0.00 | 0.00 |
| M3160 | M100 | 0.00 | 0.00 | 0.00 | 0.00 | 0.80 | 0.00 | 0.00 |
| A3161 | A101 | 20.51 | 21.00 | 16.55 | 25.14 | 21.92 | 23.17 | 18.64 |
| N3162 | N102 | 16.07 | 21.00 | 11.17 | 13.43 | 15.67 | 13.31 | 33.97 |
| **Q3163** | A103 | 43.80 | 51.94 | 43.06 | 34.74 | 58.89 | 36.76 | 19.96 |
| **N3169** | G109 | 17.85 | 7.14 | 16.55 | 28.62 | 24.23 | 14.73 | 0.00 |
| Q3171 | Q111 | 20.30 | 23.90 | 22.85 | 25.00 | 25.23 | 24.31 | 13.16 |
| **V3173** | F113 | 1.89 | 7.85 | 0.00 | 13.83 | 9.11 | 8.48 | 19.57 |
| **H3181** | W121 | 0.00 | 0.00 | 20.33 | 0.00 | 0.00 | 11.65 | 25.83 |
| L3182 | L122 | 10.33 | 5.96 | 11.17 | 7.20 | 10.02 | 14.08 | 19.88 |
| K3185 | K125 | 5.66 | 14.05 | 13.34 | 0.00 | 14.83 | 7.38 | 0.00 |
| H3186 | H126 | 19.36 | 19.07 | 16.85 | 11.92 | 23.29 | 17.59 | 19.92 |

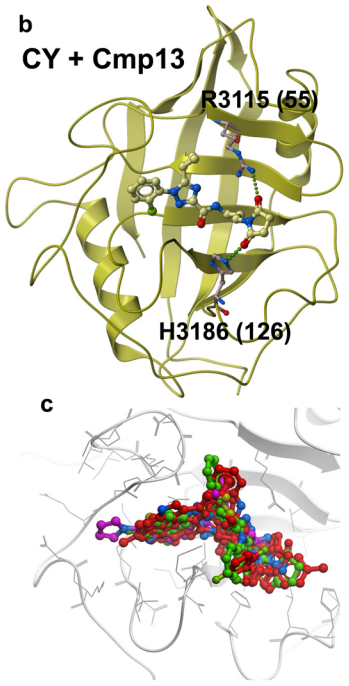


**Figure 7.** Structural poses of CY−ligand complexes. (a) Surface contact areas (Å$^2$) between docked ligands of CY and residues of PPIase pocket of CY determined by molecular modeling with ICM. Counterpart residues in CyPA are also shown (2nd column). Nonconserved residues in CY are shown in bold. Contact areas (Å$^2$) between docked CsA and residues of PPIase pocket of CyPA as determined by X-ray crystallography are shown (last column). Numbers in red denote residues establishing interactions with chemical probes identified by this study that are known not to participate in interactions between CyPA and CsA. Residues in bold are unique to CY of Ranbp2. Residues in green establish hydrogen bonds with compound **13**. (b) Hydrogen bonding between compound **13** and the conserved residues, R3115 and H3186, of the PPIase pocket of CY. Numbers in parentheses are counterpart residues in CyPA. (c) Superposition of ligands of PPIase pocket of CY; compound **11** (purple) protrudes out the PPIase pocket of CY.

all the contact areas between the residues of CY and functional groups of ligands and compared these to the crystal structure of the CyPA−CsA complex (PBD 1CWA).[70] As shown in Figure 7a, compound **11**, which presents dual activities for STAT3 and hnRNPA2B1, is predicted to interact with highest number of residues (seven) which do not interact with CsA in CyPA. Compounds **10** and **11** share pharmacological properties and sixteen interacting residues. Among these residues, five do not interact with CsA in CyPA and three (D3131, Q3163 and N3169) are not conserved in CyPA. Strikingly, compound **13**, which suppresses CY PPIase activity, is the only compound that is predicted to establish hydrogen bonds with the highly conserved residues R3115 (R55 in CyPA) and H3186, whereas a single hydrogen bond is established between all other compounds and R3115 (Figure 7b). Finally, compound **11** has an extended configuration compared with all other compounds by protruding out of the PPIase pocket toward D3141, K3142, and N3169 (Figure 7c).

## CONCLUSIONS

This study identified the first known chemical ligands with relative potency and selectivity toward CY of Ranbp2 and with idiosyncratic activities toward the modulation of the proteostasis of physiological substrates of CY, such as STAT3, hnRNPA2B1, and M-opsin. Specifically, this study found that compound **2** enhances STAT3-transcriptional activation without affecting hnRNPA2B1 proteostasis, whereas compounds **12** and **13** down-regulate hnRNPA2B1 proteostasis without affecting STAT3-transcriptional activation. Further, compounds **2** and **13** promote also mild down-regulation and up-regulation of M-opsin proteostasis, respectively. No chemical enhancers of STAT3 activity are known to this date.[48] Likewise, chemical regulators of hnRNPA2B1 and M-opsin proteostasis are elusive. Regulation of STAT3 activity is important in clinical conditions, such as cancer and neurodegeneration, promoted by intrinsic and extrinsic pathological stressors and in which activated STAT3 is thought to act as an early prosurvival factor.[48−54,71] A potential concern is whether an enhancement of prosurvival responses caused by activated STAT3 alone promotes oncogenesis in neurodegenerative therapies. However, this concern is mitigated by recent data supporting that therapeutic augmentation by activated STAT3 promotes photoreceptor survival and delays degeneration of photoreceptors across various inherited models of photoreceptor dystrophies and without apparent transformation of retinal neurons.[55] Hence, pharmacological enhancers of STAT3 activity may boost the prosurvival potential of STAT3 across multiple neurodegenerative conditions. On the other hand, human mutations in prion-like domains of hnRNPA2B1 cause MSPs and ALS,[56] whereas mutations in M-opsin compromise cone photoreceptor neural function and promote color blindness.[57] These mutations are thought to promote the misfolding or aggregation of cytotoxic hnRNPA2B1 and opsin conformers.[56,72] In this regard, this study opens new venues for the pharmacological down-regulation of disease-relevant substrates when pathological accumulations or aggregation of conformational and kinetically trapped folded substrates compromise neural survival. Finally, emerging data also support that hnRNPA2B1 is a driving oncogene in glioblastoma and that hnRNPA2B1 knockdown is accompanied by a reduction of


DOI: 10.1021/acschemneuro.5b00134
ACS Chem. Neurosci. 2015, 6, 1476−1485

activated STAT3 and transformation potential.[73,74] Hence, the chemical compounds herein uncovered may have therapeutic applications in other diseases, such as glioblastomas with overexpression of hnRNPA2B1.

This study also shows that the regulation of chaperone and PPIase activities of cyclophilins may undergo a higher level of complexity than hitherto appreciated. Our prior work showed that the mutation R3115A (R55 in CyPA), which causes the loss of PPIase activity of CY, led to the selective post-transcriptional down-regulation of hnRNPA2B1 without apparently affecting STAT3 proteostasis.[26] By contrast, this study shows that compound **13**, which also selectively inhibits the PPIase of CY and down-regulates hnRNPA2B1, shares similar pharmacological properties with compounds **10**−**12**, which have no inhibitory effect on CY PPIase activity. Assuming that these compounds maintain similar bioactive conformations *in vitro* and *in vivo*, the data indicate that loss of PPIase activity alone may not account for the down-regulation of hnRNPA2B1. Further, compound **13** is predicted to be anchored by hydrogen bonding to highly conserved residues among cyclophilins, such as H3186 (H126 in CyPA) and the catalytic residue R3115A (R55 in CyPA). Hence, it is likely that unique interactions of shared and unique residues of CY with compounds **10**−**13**, but not CsA, may contribute significantly to their unique pharmacological properties and that CY presents allosteric coupling of PPIase and chaperone activities. This ligand-elicited allosterism at the PPIase pocket may promote long-range chemical shifts in CY and the generation of CY conformers with distinct chaperone propensities toward STAT3, hnRNPA2B1, and M-opsin. Ultimately, X-ray crystal structures of chemical ligand−CY complexes, ligand structure−activity relationships, and chemical-genetic complementation studies are needed to gain additional insights into the mechanisms underpinning the pharmacological regulation of CY by the novel aforementioned compounds.

Another surprising observation was that we did not observe changes in latent and activated STAT3 levels by compounds that enhance STAT3-transcriptional activation and that compound **13** with CY PPIase inhibitory activity had no effect on STAT3-transcriptional activation. Although these pharmacological and prior results support a lack of physiological effects of *cis*−*trans* prolyl isomerization in STAT3 proteostasis and STAT3 association to Ranbp2,[26] they suggest a model whereby CY chaperones and boosts the *trans*-activation potential of STAT3 by sampling dynamic conformational substates of activated STAT3 and shifting the equilibrium between these substates to favor the formation of STAT3 conformer(s) with high *trans*-activation potential or nuclear translocation efficiencies.

Pharmacological regulation of protein−protein interactions is often viewed as difficult to target owing to large and flat interfaces between interacting partners.[75] However, small molecule-mediated allosteric (induced-fit) regulation of protein interacting interfaces may produce dynamic shifts in pre-existing and nearly isoenergetic ground conformational substates that are linked to distinct functional properties of a protein. This concept was introduced first by Linderstrøm-Lang and Schellman[76] and extended by Monod et al. to multisubunit proteins[77] and more recently to "single-domain" proteins,[78−80] including cyclophilins.[59,61] We suggest that the dynamic interconversion of functionally and structurally distinct ensembles may not only underlie chaperone activity through the adaptive recognition of client proteins but have also critical implications to the allosteric regulation of bidirectional transport of substrates through the nuclear pore. Oscillations in conformational substates of CY (and other domains)[43] of Ranbp2 and exclusive association of selective conformers to import (e.g., STAT3) or export substrates (e.g., hnRNPA2B1) may contribute to the directionality of nucleocytoplasmic trafficking and protestasis of client proteins. In this regard, the chemical probes here discovered will help to explore pharmacologically the dynamic roles of protein conformational substates in the regulation of nucleocytoplasmic trafficking, recognition, and proteostasis of client proteins, which likely extend beyond those examined in this study, such as the capsid of HIV-1.[15,58]

## METHODS

**Virtual Ligand Screening (VLS) of MolCart Database.** The 1.75 Å resolution crystal structure of human CY of Ranbp2 (PDB code 4I9Y) was used in the virtual screen.[64] The structure was prepared for virtual screening by using standard protocols in Internal Coordinate Mechanics (ICM-Pro) software v3.8 (MolSoft's LLC, San Diego, CA).[81−83]

The MolCart Compounds database (http://www.molsoft.com/molcart-compounds.html) containing 8 932 994 commercially available chemicals was filtered using a relaxed set of "Lipinski-like" chemical drug-like property rules.[84] The database was then screened against the extended orthosteric PPIase pocket of CY of Ranbp2. VLS was performed with Internal Coordinate Mechanics-Pro (ICM-Pro VLS software v3.8) and dockScan v.4.41 (MolSoft's LLC, San Diego, CA). The ICM program performs global optimization of the entire flexible ligand in the receptor field and combines large-scale random moves of several types with gradient local minimization and a search history mechanism using the ICM biased probability Monte Carlo procedure.[81] Docking poses were evaluated according to the weighted components of the ICM-VLS scoring function,[85] which gives a good approximation of the binding free energy between a ligand and a receptor and is a function of different energy terms based on a force field. The side chains of CY were not explicitly flexible during the screening. A soft van der Waals potential was used to allow partial flexibility between the ligand and receptor, but no large side-chain or backbone movements were incorporated. Based on the distribution of scores a scoring threshold of −37 was employed to differentiate potential binders from nonbinders. The ranked hit list was checked for compounds with unusual chemical properties (e.g., reactive and or potentially PAIN compounds[86] and high strain (e.g., *cis* amides), and these chemicals were removed. The hit list was then clustered using MolSoft's Atomic Property Field (APF) method[87] to select a diverse set of 735 chemicals for experimental testing.

The hit list was then counter-screened against the active site of CyPA\PPIA (PDB 2CPL).[66] Fifty-six of the chemicals in the final ranked hit list of CY of Ranbp2 were predicted to bind to CY of Ranbp2 and CyPA, and they were removed from the final hit list. Top scoring compounds were visually inspected, and 14 compounds were selected for experimental evaluation.

**Reagents and Antibodies.** Oncostatin-M (OncM) and interleukin 6 (IL6) were obtained from R&D Systems. Monoclonal mouse mAb414 against Nup358/Ranbp2, Nup153, and Nup62 were obtained from Convance, Emeryville, CA. Rabbit anti-L/M-opsin no. 21069[42] and rabbit polyclonal anti-hnRNPA2B1 were obtained from Proteintech, Chicago, IL. Rabbit monoclonal anti-STAT3 was obtained from Cell Signaling, Boston, MA. Rabbit anti-pSTAT3 was obtained from Cell Signaling. Mouse rabbit anti-glyceraldehyde 3-phosphate dehydrogenase (Gapdh) was obtained from Santa Cruz Biotechnology. Rabbit anti-hsc70 was obtained from Enzo Life Science, Farmingdale, NY. Bovine thymus cyclophilin A was obtained from Sigma. Suc-ALPF-*p*NA was obtained from Bachem Bioscience. Cyclosporine A (CsA) was obtained from Sigma. Bovine pancreas α-chymotrypsin type 1-S was obtained from Sigma. Purity of chemical


DOI: 10.1021/acschemneuro.5b00134
ACS Chem. Neurosci. 2015, 6, 1476−1485

compounds **1**, **2**, **10**, **11**, **12**, and **13** was 93%, 100%, 94%, 98%, 92%, and 96%, respectively, as provided by the manufacturers.

**Cell Culture.** The STAT3 luciferase reporter HeLa stable cell line (Signosis, Santa Clara, CA) was maintained in DMEM (Invitrogen) supplemented with serum inactivated fetal bovine serum (Hyclone), penicillin, and streptomycin. HeLa cells were seeded in 96-well plates (8000 cells per well) and cultured overnight at 37 °C in the presence of 5% $CO_2$ and 100% humidity. For STAT3 activation and small compound screenings, HeLA cells were then challenged for 16 h with OncM or IL-6 in 0.1% FBS and in the presence or absence of various concentrations of small compounds or CsA dissolved in anhydrous DMSO. DMSO concentration between treatments with and without compounds was kept constant. Then, luciferase assays were carried out as recommended by the manufacturer (Luciferase reporter system, Promega). Luminescence was measured with a SpectraMax M5 spectrometer plate reader (Molecular Devices). For analysis of hnRNPA2B1 and M-opsin proteostasis, HeLa cells and the murine photoreceptor cell line, 661W,[68,69] underwent the same procedures with the exception that they were grown to confluency (~1.2 million cells) in six-well plates without cytokine stimulation and in the absence or presence small compounds. Viability and cytotoxicity were assessed with ApoTox-Glo Triplex Assay (Promega), microscopic examination, and comparisons between small molecules at 250 $\mu$M and staurosporin at 5 $\mu$M. Cells were harvested and lysed in radioimmunoprecipitation assay (RIPA) buffer.

**PPIase Assays.** Recombinant CY of Ranbp2 was purified as described elsewhere.[26,88] PPIase assays for the *cis*−*trans* prolyl isomerization of Suc-ALPF-*p*NA by recombinant CY of Ranbp2 (50 nM) or thymus-purified CyPA (5 nM) were performed using the chymotrypsin-coupled assay exactly as described previously, but in the absence or presence of small compounds or CsA.[26,29] The first-order rate constants, $k$, and catalytic efficiency, $k_{cat}/K_m$, were determined with Origin software v8.5. (Northampton, MA) exactly as described previously.[26,29] The $IC_{50}$ value for CY PPIase inhibitor(s) (small compound) was ascertained using the chymotrypsin-coupled assay described above.

**Quantitative Immunoblot Analyses.** RIPA-solubilized cell homogenates were resolved in standard Hoefer (Holliston, MA) or premade 4−14% Criterion (BioRad) SDS-polyacrylamide gels. Changes in protein levels caused by compound treatments were ascertained by immunoblots and densitometric analyses as described previously.[26] Blots were reprobed for housekeeping proteins. Band intensities were quantified with Metamorph v 7.0 (Molecular Devices), and integrated density values (idv) of representative bands were normalized to the background and idv of Gapdh or hsc70. Data were analyzed by the two-tail $t$-test and a $p$ value of $\leq 0.05$ was considered significant.

## AUTHOR INFORMATION

### Corresponding Author

*Paulo A. Ferreira. Mailing address: Duke University Medical Center, DUEC 3802, 2351 Erwin Road, Durham, NC 27710. Tel: 919-684-8457. Fax: 919-684-3826. E-mail: paulo.ferreira@duke.edu.

### Funding

This work was supported by the National Institutes of Health Grants EY019492 and GM083165 to P.A.F.

### Notes

The authors declare no competing financial interest.

## ACKNOWLEDGMENTS

We thank the undergraduate summer fellows Aitana Zermeno (Howard Hughes Research Fellows Program, Duke University) and Basirul Haque (North Carolina State University) for their help with these studies.

## REFERENCES

(1) Fischer, G., Wittmann-Liebold, B., Lang, K., Kiefhaber, T., and Schmid, F. X. (1989) Cyclophilin and peptidyl-prolyl cis-trans isomerase are probably identical proteins. *Nature 337*, 476−478.

(2) Takahashi, N., Hayano, T., and Suzuki, M. (1989) Peptidyl-prolyl cis-trans isomerase is the cyclosporin A-binding protein cyclophilin. *Nature 337*, 473−475.

(3) Camilloni, C., Sahakyan, A. B., Holliday, M. J., Isern, N. G., Zhang, F., Eisenmesser, E. Z., and Vendruscolo, M. (2014) Cyclophilin A catalyzes proline isomerization by an electrostatic handle mechanism. *Proc. Natl. Acad. Sci. U. S. A. 111*, 10203−10208.

(4) Schiene-Fischer, C., Aumüller, T., and Fischer, G. (2013) Peptide Bond *cis/trans* Isomerases: A Biocatalysis Perspective of Conformational Dynamics in Proteins. *Top. Curr. Chem. 328*, 35−67.

(5) Ferreira, P. A., and Orry, A. (2012) From Drosophila to humans: Reflections on the roles of the prolyl isomerases and chaperones, cyclophilins, in cell function and disease. *J. Neurogenet. 26*, 132−143.

(6) Lu, K. P., Finn, G., Lee, T. H., and Nicholson, L. K. (2007) Prolyl cis-trans isomerization as a molecular timer. *Nat. Chem. Biol. 3*, 619−629.

(7) Handschumacher, R. E., Harding, M. W., Rice, J., Drugge, R. J., and Speicher, D. W. (1984) Cyclophilin: A specific cytosolic binding protein for cyclosporin A. *Science 226*, 544−547.

(8) Colgan, J., Asmal, M., Yu, B., and Luban, J. (2005) Cyclophilin A-deficient mice are resistant to immunosuppression by cyclosporine. *J. Immunol. 174*, 6030−6038.

(9) Galat, A., and Bua, J. (2010) Molecular aspects of cyclophilins mediating therapeutic actions of their ligands. *Cell. Mol. Life Sci. 67*, 3467−3488.

(10) Schreiber, S. L. (1991) Chemistry and biology of the immunophilins and their immunosuppressive ligands. *Science 251*, 283−287.

(11) Edlich, F., and Fischer, G. (2006) Pharmacological targeting of catalyzed protein folding: The example of peptide bond cis/trans isomerases. *Handb. Exp. Pharmacol.*, 359−404.

(12) Gerard, M., Deleersnijder, A., Demeulemeester, J., Debyser, Z., and Baekelandt, V. (2011) Unraveling the role of peptidyl-prolyl isomerases in neurodegeneration. *Mol. Neurobiol. 44*, 13−27.

(13) Dorner, M., Horwitz, J. A., Donovan, B. M., Labitt, R. N., Budell, W. C., Friling, T., Vogt, A., Catanese, M. T., Satoh, T., Kawai, T., Akira, S., Law, M., Rice, C. M., and Ploss, A. (2013) Completion of the entire hepatitis C virus life cycle in genetically humanized mice. *Nature 501*, 237−241.

(14) Coelmont, L., Hanoulle, X., Chatterji, U., Berger, C., Snoeck, J., Bobardt, M., Lim, P., Vliegen, I., Paeshuyse, J., Vuagniaux, G., Vandamme, A. M., Bartenschlager, R., Gallay, P., Lippens, G., and Neyts, J. (2010) DEB025 (Alisporivir) inhibits hepatitis C virus replication by preventing a cyclophilin A induced cis-trans isomerisation in domain II of NS5A. *PLoS One 5*, No. e13687.

(15) Schaller, T., Ocwieja, K. E., Rasaiyaah, J., Price, A. J., Brady, T. L., Roth, S. L., Hue, S., Fletcher, A. J., Lee, K., KewalRamani, V. N., Noursadeghi, M., Jenner, R. G., James, L. C., Bushman, F. D., and Towers, G. J. (2011) HIV-1 capsid-cyclophilin interactions determine nuclear import pathway, integration targeting and replication efficiency. *PLoS Pathol. 7*, No. e1002439.

(16) Franke, E. K., and Luban, J. (1996) Inhibition of HIV-1 replication by cyclosporine A or related compounds correlates with the ability to disrupt the Gag-cyclophilin A interaction. *Virology 222*, 279−282.

(17) Rasaiyaah, J., Tan, C. P., Fletcher, A. J., Price, A. J., Blondeau, C., Hilditch, L., Jacques, D. A., Selwood, D. L., James, L. C., Noursadeghi, M., and Towers, G. J. (2013) HIV-1 evades innate immune recognition through specific cofactor recruitment. *Nature 503*, 402−405.

(18) Lin, K., and Gallay, P. (2013) Curing a viral infection by targeting the host: The example of cyclophilin inhibitors. *Antiviral Res. 99*, 68−77.

(19) Schneuwly, S., Shortridge, R. D., Larrivee, D. C., Ono, T., Ozaki, M., and Pak, W. L. (1989) *Drosophila* ninaA gene encodes an eye-



DOI: 10.1021/acschemneuro.5b00134
*ACS Chem. Neurosci.* 2015, 6, 1476−1485

specific cyclophilin (cyclosporine A binding protein). *Proc. Natl. Acad. Sci. U. S. A. 86*, 5390−5394.
(20) Shieh, B. H., Stamnes, M. A., Seavello, S., Harris, G. L., and Zuker, C. S. (1989) The ninaA gene required for visual transduction in *Drosophila* encodes a homologue of cyclosporin A-binding protein. *Nature 338*, 67−70.
(21) Baker, E. K., Colley, N. J., and Zuker, C. S. (1994) The cyclophilin homolog NinaA functions as a chaperone, forming a stable complex in vivo with its protein target rhodopsin. *EMBO J. 13*, 4886−4895.
(22) Ingelfinger, D., Gothel, S. F., Marahiel, M. A., Reidt, U., Ficner, R., Luhrmann, R., and Achsel, T. (2003) Two protein-protein interaction sites on the spliceosome-associated human cyclophilin CypH. *Nucleic Acids Res. 31*, 4791−4796.
(23) Xu, C., Zhang, J., Huang, X., Sun, J., Xu, Y., Tang, Y., Wu, J., Shi, Y., Huang, Q., and Zhang, Q. (2006) Solution structure of human peptidyl prolyl isomerase-like protein 1 and insights into its interaction with SKIP. *J. Biol. Chem. 281*, 15900−15908.
(24) Reidt, U., Wahl, M. C., Fasshauer, D., Horowitz, D. S., Luhrmann, R., and Ficner, R. (2003) Crystal structure of a complex between human spliceosomal cyclophilin H and a U4/U6 snRNP-60K peptide. *J. Mol. Biol. 331*, 45−56.
(25) Ishikawa, Y., Vranka, J. A., Boudko, S. P., Pokidysheva, E., Mizuno, K., Zientek, K., Keene, D. R., Rashmir-Raven, A. M., Nagata, K., Winand, N. J., and Bachinger, H. P. (2012) Mutation in cyclophilin B that causes hyperelastosis cutis in American Quarter Horse does not affect peptidylprolyl cis-trans isomerase activity but shows altered cyclophilin B-protein interactions and affects collagen folding. *J. Biol. Chem. 287*, 22253−22265.
(26) Cho, K. I., Patil, H., Senda, E., Wang, J., Yi, H., Qiu, S., Yoon, D., Yu, M., Orry, A., Peachey, N. S., and Ferreira, P. A. (2014) Differential Loss of Prolyl Isomerase or Chaperone Activity of Ran-binding Protein 2 (Ranbp2) Unveils Distinct Physiological Roles of Its Cyclophilin Domain in Proteostasis. *J. Biol. Chem. 289*, 4600−4625.
(27) Wu, J., Matunis, M. J., Kraemer, D., Blobel, G., and Coutavas, E. (1995) Nup358, a cytoplasmically exposed nucleoporin with peptide repeats, Ran-GTP binding sites, zinc fingers, a cyclophilin A homologous domain, and a leucine-rich region. *J. Biol. Chem. 270*, 14209−14213.
(28) Yokoyama, N., Hayashi, N., Seki, T., Pante, N., Ohba, T., Nishii, K., Kuma, K., Hayashida, T., Miyata, T., Aebi, U., et al. (1995) A giant nucleopore protein that binds Ran/TC4. *Nature 376*, 184−188.
(29) Ferreira, P. A., Hom, J. T., and Pak, W. L. (1995) Retina-specifically expressed novel subtypes of bovine cyclophilin. *J. Biol. Chem. 270*, 23179−23188.
(30) Mavlyutov, T. A., Cai, Y., and Ferreira, P. A. (2002) Identification of RanBP2- and Kinesin-Mediated Transport Pathways with Restricted Neuronal and Subcellular Localization. *Traffic 3*, 630−640.
(31) Delphin, C., Guan, T., Melchior, F., and Gerace, L. (1997) RanGTP targets p97 to RanBP2, a filamentous protein localized at the cytoplasmic periphery of the nuclear pore complex. *Mol. Biol. Cell 8*, 2379−2390.
(32) Vetter, I. R., Nowak, C., Nishimoto, T., Kuhlmann, J., and Wittinghofer, A. (1999) Structure of a Ran-binding domain complexed with Ran bound to a GTP analogue: Implications for nuclear transport. *Nature 398*, 39−46.
(33) Hamada, M., Haeger, A., Jeganathan, K. B., van Ree, J. H., Malureanu, L., Walde, S., Joseph, J., Kehlenbach, R. H., and van Deursen, J. M. (2011) Ran-dependent docking of importin-beta to RanBP2/Nup358 filaments is essential for protein import and cell viability. *J. Cell Biol. 194*, 597−612.
(34) Walde, S., Thakar, K., Hutten, S., Spillner, C., Nath, A., Rothbauer, U., Wiemann, S., and Kehlenbach, R. H. (2012) The nucleoporin Nup358/RanBP2 promotes nuclear import in a cargo- and transport receptor-specific manner. *Traffic 13*, 218−233.
(35) Packham, S., Warsito, D., Lin, Y., Sadi, S., Karlsson, R., Sehat, B., and Larsson, O. (2015) Nuclear translocation of IGF-1R via p150(Glued) and an importin-beta/RanBP2-dependent pathway in cancer cells. *Oncogene 34*, 2227−2238.
(36) Frohnert, C., Hutten, S., Walde, S., Nath, A., and Kehlenbach, R. H. (2014) Importin 7 and Nup358 promote nuclear import of the protein component of human telomerase. *PLoS One 9*, No. e88887.
(37) Singh, B. B., Patel, H. H., Roepman, R., Schick, D., and Ferreira, P. A. (1999) The zinc finger cluster domain of RanBP2 is a specific docking site for the nuclear export factor, exportin-1. *J. Biol. Chem. 274*, 37370−37378.
(38) Werner, A., Flotho, A., and Melchior, F. (2012) The RanBP2/RanGAP1(*)SUMO1/Ubc9 Complex Is a Multisubunit SUMO E3 Ligase. *Mol. Cell 46*, 287−298.
(39) Pichler, A., Gast, A., Seeler, J. S., Dejean, A., and Melchior, F. (2002) The nucleoporin RanBP2 has SUMO1 E3 ligase activity. *Cell 108*, 109−120.
(40) Saitoh, H., Sparrow, D. B., Shiomi, T., Pu, R. T., Nishimoto, T., Mohun, T. J., and Dasso, M. (1998) Ubc9p and the conjugation of SUMO-1 to RanGAP1 and RanBP2. *Curr. Biol. 8*, 121−124.
(41) Cai, Y., Singh, B. B., Aslanukov, A., Zhao, H., and Ferreira, P. A. (2001) The docking of kinesins, KIF5B and KIF5C, to Ran-binding protein 2 (RanBP2) is mediated via a novel RanBP2 domain. *J. Biol. Chem. 276*, 41594−41602.
(42) Cho, K. I., Cai, Y., Yi, H., Yeh, A., Aslanukov, A., and Ferreira, P. A. (2007) Association of the Kinesin-Binding Domain of RanBP2 to KIF5B and KIF5C Determines Mitochondria Localization and Function. *Traffic 8*, 1722−1735.
(43) Cho, K. I., Yi, H., Desai, R., Hand, A. R., Haas, A. L., and Ferreira, P. A. (2009) RANBP2 is an allosteric activator of the conventional kinesin-1 motor protein, KIF5B, in a minimal cell-free system. *EMBO Rep. 10*, 480−486.
(44) Ferreira, P. A., Nakayama, T. A., Pak, W. L., and Travis, G. H. (1996) Cyclophilin-related protein RanBP2 acts as chaperone for red/green opsin. *Nature 383*, 637−640.
(45) Ferreira, P. A., Nakayama, T. A., and Travis, G. H. (1997) Interconversion of red opsin isoforms by the cyclophilin-related chaperone protein Ran-binding protein 2. *Proc. Natl. Acad. Sci. U. S. A. 94*, 1556−1561.
(46) Yi, H., Friedman, J. L., and Ferreira, P. A. (2007) The cyclophilin-like domain of Ran-binding protein-2 modulates selectively the activity of the ubiquitin-proteasome system and protein biogenesis. *J. Biol. Chem. 282*, 34770−34778.
(47) Ferreira, P. A., Yunfei, C., Schick, D., and Roepman, R. (1998) The cyclophilin-like domain mediates the association of Ran-binding protein 2 with subunits of the 19 S regulatory complex of the proteasome. *J. Biol. Chem. 273*, 24676−24682.
(48) Miklossy, G., Hilliard, T. S., and Turkson, J. (2013) Therapeutic modulators of STAT signalling for human diseases. *Nat. Rev. Drug Discovery 12*, 611−629.
(49) O'Shea, J. J., Holland, S. M., and Staudt, L. M. (2013) JAKs and STATs in immunity, immunodeficiency, and cancer. *N. Engl. J. Med. 368*, 161−170.
(50) Yu, H., Pardoll, D., and Jove, R. (2009) STATs in cancer inflammation and immunity: A leading role for STAT3. *Nat. Rev. Cancer 9*, 798−809.
(51) Burda, J. E., and Sofroniew, M. V. (2014) Reactive gliosis and the multicellular response to CNS damage and disease. *Neuron 81*, 229−248.
(52) Samardzija, M., Wenzel, A., Aufenberg, S., Thiersch, M., Reme, C., and Grimm, C. (2006) Differential role of Jak-STAT signaling in retinal degenerations. *FASEB J. 20*, 2411−2413.
(53) Schaeferhoff, K., Michalakis, S., Tanimoto, N., Fischer, M. D., Becirovic, E., Beck, S. C., Huber, G., Rieger, N., Riess, O., Wissinger, B., Biel, M., Seeliger, M. W., and Bonin, M. (2010) Induction of STAT3-related genes in fast degenerating cone photoreceptors of cpfl1 mice. *Cell. Mol. Life Sci. 67*, 3173−3186.
(54) Ozawa, Y., Nakao, K., Kurihara, T., Shimazaki, T., Shimmura, S., Ishida, S., Yoshimura, A., Tsubota, K., and Okano, H. (2008) Roles of STAT3/SOCS3 pathway in regulating the visual function and


DOI: 10.1021/acschemneuro.5b00134
*ACS Chem. Neurosci.* 2015, 6, 1476−1485

ubiquitin-proteasome-dependent degradation of rhodopsin during retinal inflammation. *J. Biol. Chem. 283*, 24561−24570.
(55) Jiang, K., Wright, K. L., Zhu, P., Szego, M. J., Bramall, A. N., Hauswirth, W. W., Li, Q., Egan, S. E., and McInnes, R. R. (2014) STAT3 promotes survival of mutant photoreceptors in inherited photoreceptor degeneration models. *Proc. Natl. Acad. Sci. U. S. A. 111*, E5716−5723.
(56) Kim, H. J., Kim, N. C., Wang, Y. D., Scarborough, E. A., Moore, J., Diaz, Z., MacLea, K. S., Freibaum, B., Li, S., Molliex, A., Kanagaraj, A. P., Carter, R., Boylan, K. B., Wojtas, A. M., Rademakers, R., Pinkus, J. L., Greenberg, S. A., Trojanowski, J. Q., Traynor, B. J., Smith, B. N., Topp, S., Gkazi, A. S., Miller, J., Shaw, C. E., Kottlors, M., Kirschner, J., Pestronk, A., Li, Y. R., Ford, A. F., Gitler, A. D., Benatar, M., King, O. D., Kimonis, V. E., Ross, E. D., Weihl, C. C., Shorter, J., and Taylor, J. P. (2013) Mutations in prion-like domains in hnRNPA2B1 and hnRNPA1 cause multisystem proteinopathy and ALS. *Nature 495*, 467−473.
(57) Gardner, J. C., Webb, T. R., Kanuga, N., Robson, A. G., Holder, G. E., Stockman, A., Ripamonti, C., Ebenezer, N. D., Ogun, O., Devery, S., Wright, G. A., Maher, E. R., Cheetham, M. E., Moore, A. T., Michaelides, M., and Hardcastle, A. J. (2010) X-linked cone dystrophy caused by mutation of the red and green cone opsins. *Am. J. Hum. Genet. 87*, 26−39.
(58) Bichel, K., Price, A. J., Schaller, T., Towers, G. J., Freund, S. M., and James, L. C. (2013) HIV-1 capsid undergoes coupled binding and isomerization by the nuclear pore protein NUP358. *Retrovirology 10*, 81.
(59) Fraser, J. S., Clarkson, M. W., Degnan, S. C., Erion, R., Kern, D., and Alber, T. (2009) Hidden alternative structures of proline isomerase essential for catalysis. *Nature 462*, 669−673.
(60) Ramanathan, A., Savol, A. J., Langmead, C. J., Agarwal, P. K., and Chennubhotla, C. S. (2011) Discovering conformational sub-states relevant to protein function. *PLoS One 6*, No. e15827.
(61) Burnley, B. T., Afonine, P. V., Adams, P. D., and Gros, P. (2012) Modelling dynamics in protein crystal structures by ensemble refinement. *Elife 1*, No. e00311.
(62) Liu, J., Chen, C. M., and Walsh, C. T. (1991) Human and *Escherichia coli* cyclophilins: Sensitivity to inhibition by the immunosuppressant cyclosporin A correlates with a specific tryptophan residue. *Biochemistry (Moscow) 30*, 2306−2310.
(63) Hoffmann, K., Kakalis, L. T., Anderson, K. S., Armitage, I. M., and Handschumacher, R. E. (1995) Expression of human cyclophilin-40 and the effect of the His141−>Trp mutation on catalysis and cyclosporin A binding. *Eur. J. Biochem. 229*, 188−193.
(64) Lin, D. H., Zimmermann, S., Stuwe, T., Stuwe, E., and Hoelz, A. (2013) Structural and functional analysis of the C-terminal domain of Nup358/RanBP2. *J. Mol. Biol. 425*, 1318−1329.
(65) Lammers, M., Neumann, H., Chin, J. W., and James, L. C. (2010) Acetylation regulates cyclophilin A catalysis, immunosuppression and HIV isomerization. *Nat. Chem. Biol. 6*, 331−337.
(66) Ke, H. (1992) Similarities and differences between human cyclophilin A and other beta-barrel structures. Structural refinement at 1.63 A resolution. *J. Mol. Biol. 228*, 539−550.
(67) Bauer, K., Kretzschmar, A. K., Cvijic, H., Blumert, C., Loffler, D., Brocke-Heidrich, K., Schiene-Fischer, C., Fischer, G., Sinz, A., Clevenger, C. V., and Horn, F. (2009) Cyclophilins contribute to Stat3 signaling and survival of multiple myeloma cells. *Oncogene 28*, 2784−2795.
(68) al-Ubaidi, M. R., Font, R. L., Quiambao, A. B., Keener, M. J., Liou, G. I., Overbeek, P. A., and Baehr, W. (1992) Bilateral retinal and brain tumors in transgenic mice expressing simian virus 40 large T antigen under control of the human interphotoreceptor retinoid-binding protein promoter. *J. Cell Biol. 119*, 1681−1687.
(69) Tan, E., Ding, X. Q., Saadi, A., Agarwal, N., Naash, M. I., and Al-Ubaidi, M. R. (2004) Expression of cone-photoreceptor-specific antigens in a cell line derived from retinal tumors in transgenic mice. *Invest. Ophthalmol. Vis. Sci. 45*, 764−768.
(70) Mikol, V., Kallen, J., Pflugl, G., and Walkinshaw, M. D. (1993) X-ray structure of a monomeric cyclophilin A-cyclosporin A crystal complex at 2.1 A resolution. *J. Mol. Biol. 234*, 1119−1130.
(71) Xia, X., Li, Y., Huang, D., Wang, Z., Luo, L., Song, Y., Zhao, L., and Wen, R. (2011) Oncostatin M protects rod and cone photoreceptors and promotes regeneration of cone outer segment in a rat model of retinal degeneration. *PLoS One 6*, No. e18282.
(72) Noorwez, S. M., Kuksa, V., Imanishi, Y., Zhu, L., Filipek, S., Palczewski, K., and Kaushal, S. (2003) Pharmacological chaperone-mediated in vivo folding and stabilization of the P23H-opsin mutant associated with autosomal dominant retinitis pigmentosa. *J. Biol. Chem. 278*, 14442−14450.
(73) Deng, J., Chen, S., Wang, F., Zhao, H., Xie, Z., Xu, Z., Zhang, Q., Liang, P., Zhai, X., and Cheng, Y. (2015) Effects of hnRNP A2/B1 Knockdown on Inhibition of Glioblastoma Cell Invasion, Growth and Survival. *Mol. Neurobiol.*, DOI: 10.1007/s12035-014-9080-3.
(74) Golan-Gerstl, R., Cohen, M., Shilo, A., Suh, S. S., Bakacs, A., Coppola, L., and Karni, R. (2011) Splicing factor hnRNP A2/B1 regulates tumor suppressor gene splicing and is an oncogenic driver in glioblastoma. *Cancer Res. 71*, 4464−4472.
(75) Arkin, M. R., Tang, Y., and Wells, J. A. (2014) Small-molecule inhibitors of protein-protein interactions: progressing toward the reality. *Chem. Biol. 21*, 1102−1114.
(76) Linderstrøm-Lang, K., and Schellman, J. A. (1959) Protein structure and enzyme activity, in *The Enzymes* (Boyer, P. D., Lardy, H., and Myrback, K., Eds.) 2nd ed., pp 443−510, Academic Press, New York.
(77) Monod, J., Wyman, J., and Changeux, J. P. (1965) On the Nature of Allosteric Transitions: A Plausible Model. *J. Mol. Biol. 12*, 88−118.
(78) Volkman, B. F., Lipson, D., Wemmer, D. E., and Kern, D. (2001) Two-state allosteric behavior in a single-domain signaling protein. *Science 291*, 2429−2433.
(79) Tsai, C. J., Del Sol, A., and Nussinov, R. (2009) Protein allostery, signal transmission and dynamics: A classification scheme of allosteric mechanisms. *Mol. Biosyst. 5*, 207−216.
(80) Li, P., Martins, I. R., Amarasinghe, G. K., and Rosen, M. K. (2008) Internal dynamics control activation and activity of the autoinhibited Vav DH domain. *Nat. Struct. Mol. Biol. 15*, 613−618.
(81) Abagyan, R., and Totrov, M. (1994) Biased probability Monte Carlo conformational searches and electrostatic calculations for peptides and proteins. *J. Mol. Biol. 235*, 983−1002.
(82) Abagyan, R., Totrov, M., and Kuznetsov, D. (1994) ICM-a new method for protein modeling and design: Applications to docking and structure prediction from the distorted native conformation. *J. Comput. Chem. 15*, 488−506.
(83) Orry, A. J., and Abagyan, R. (2012) Preparation and refinement of model protein-ligand complexes. *Methods Mol. Biol. 857*, 351−373.
(84) Lipinski, C. A., Lombardo, F., Dominy, B. W., and Feeney, P. J. (2001) Experimental and computational approaches to estimate solubility and permeability in drug discovery and development settings. *Adv. Drug Delivery Rev. 46*, 3−26.
(85) Totrov, M., and Abagyan, R. (1999) Derivation of sensitive discrimination potential for virtual ligand screening, in *Third Annual International Conference on Computational Molecular Biology*, pp 312−320, Association for Computing Machinery, Lyon, France.
(86) Baell, J. B., and Holloway, G. A. (2010) New substructure filters for removal of pan assay interference compounds (PAINS) from screening libraries and for their exclusion in bioassays. *J. Med. Chem. 53*, 2719−2740.
(87) Totrov, M. (2008) Atomic property fields: Generalized 3D pharmacophoric potential for automated ligand superposition, pharmacophore elucidation and 3D QSAR. *Chem. Biol. Drug Des. 71*, 15−27.
(88) Ferreira, P. A. (2000) Characterization of RanBP2-associated molecular components in neuroretina. *Methods Enzymol. 315*, 455−468.


DOI: 10.1021/acschemneuro.5b00134
*ACS Chem. Neurosci.* 2015, 6, 1476−1485